Soft Matter

Molecularly-ordered hydrogels with controllable, anisotropic stimulus response

Journal:	*Soft Matter*
Manuscript ID	SM-ART-04-2019-000763.R1
Article Type:	Paper
Date Submitted by the Author:	30-Apr-2019
Complete List of Authors:	Boothby, Jennifer; The University of Texas at Dallas, Bioengineering Samuel, Jeremy; The University of Texas at Dallas, Bioengineering Ware, Taylor; The University of Texas at Dallas, Bioengineering

ARTICLE

Molecularly-ordered hydrogels with controllable, anisotropic stimulus response

Received 00th January 20xx,
Accepted 00th January 20xx

DOI: 10.1039/x0xx00000x

Jennifer M. Boothby[a], Jeremy Samuel[a], and Taylor H. Ware*[a]

Hydrogels which morph between programmed shapes in response to aqueous stimuli are of significant interest for biosensors and artificial muscles, among other applications. However, programming hydrogel shape change at small size scales is a significant challenge. Here we use the inherent ordering capabilities of liquid crystals to create a mechanically anisotropic hydrogel; when coupled with responsive comonomers, the mechanical anisotropy in the network guides shape change in response to the desired aqueous condition. Our synthetic strategy hinges on the use of a methacrylic chromonic liquid crystal monomer which can be combined with a non-polymerizable chromonic of similar structure to vary the magnitude of shape change while retaining liquid crystalline order. This shape change is directional due to the mechanical anisotropy of the gel, which is up to 50% stiffer along the chromonic stack direction than perpendicular. Additionally, we show that the type of stimulus to which these anisotropic gels respond can be switched by incorporating responsive, hydrophilic comonomers without destroying the nematic phase or alignment. The utility of these properties is demonstrated in polymerized microstructures which exhibit Gaussian curvature due to emergent ordering in a micron-sized capillary in response to low pH.

Introduction

Smart hydrogels which actuate in response to fluctuations in aqueous conditions are a promising tool for biosensors, tissue scaffolds, drug delivery devices, and microfluidics.[1–9] The functions of these actuating hydrogels are often dependent on range of size scales over which shape change can be programmed, often limited by manufacturing methods. Most hydrogels are isotropic materials, which result in uniform volume change in all directions upon swelling. Where complex shape change is required, shape change can be controlled by spatially controlling either the magnitude or anisotropy of swelling. Directing shape change spatially in hydrogels can allow complex shape change for multiple functions.

Shape programming in hydrogels is most commonly achieved by spatially varying either the material or the processing. Composite hydrogels leverage multiple materials with different swelling or mechanical properties to yield a controlled shape change.[10–12] One way to spatially vary material is to laminate the hydrogel with a stiffer layer. For example, by patterning periodic angled strips of stiff polymer in a soft polymer sheet, a helix can be programmed to emerge upon swelling in water.[13] Another way to program shape in heterogenous materials is to embed a stiff particulate, such as carbon nanotubes, cellulose nanocrystals and nanofibers, or metallic nanosheets to create a global anisotropy which can guide shape change.[14–17] These strategies can be readily used to control shape morphing, but the size scale of the actuator is limited by the method used to process the composite.

In a monolithic polymer, one way to achieve heterogeneous swelling is by varying the crosslink density within a material. This is typically done by selective exposure to light-sensitive crosslinkers.[18,19] However, the size scale of these actuators is limited by the top-down photopatterning step. Anisotropic networks in monolithic materials can be formed by directional freezing. Directional freezing has been used to generate aligned porous networks in water-soluble polymers.[20–22] However, with this approach, the architecture cannot be readily programmed in a spatially directed manner.

Locally anisotropic networks can also be synthesized by leveraging liquid crystalline order in polymer networks. Liquid crystals are anisotropic molecules whose orientation can be controlled in the liquid crystalline phase, often by mechanical shearing or through interactions with patterned surfaces.[23–27] Elastomers and glassy polymer networks with liquid crystalline order exhibit anisotropic mechanical properties which are up to six times stiffer along the direction of alignment versus perpendicular to the alignment.[28,29] However, significantly fewer hydrogels with liquid crystalline order have been demonstrated, as polymerizable liquid crystals are typically hydrophobic molecules. Lyotropic liquid crystals are amphiphilic molecules which self-assemble in a concentration-dependent manner in aqueous solutions. The directionality of these assemblies is difficult to manipulate, and the configurations are often limited. Anisotropic polymer networks from lyotropic liquid crystals have been synthesized where the network architecture is controlled only by the concentration-dependent phase of the liquid crystal.[30–33] However, spatially

[a] The University of Texas at Dallas, 800 W. Campbell Rd, Richardson, TX, 75080
Electronic Supplementary Information (ESI) available: [details of any supplementary information available should be included here]. See DOI: 10.1039/x0xx00000x

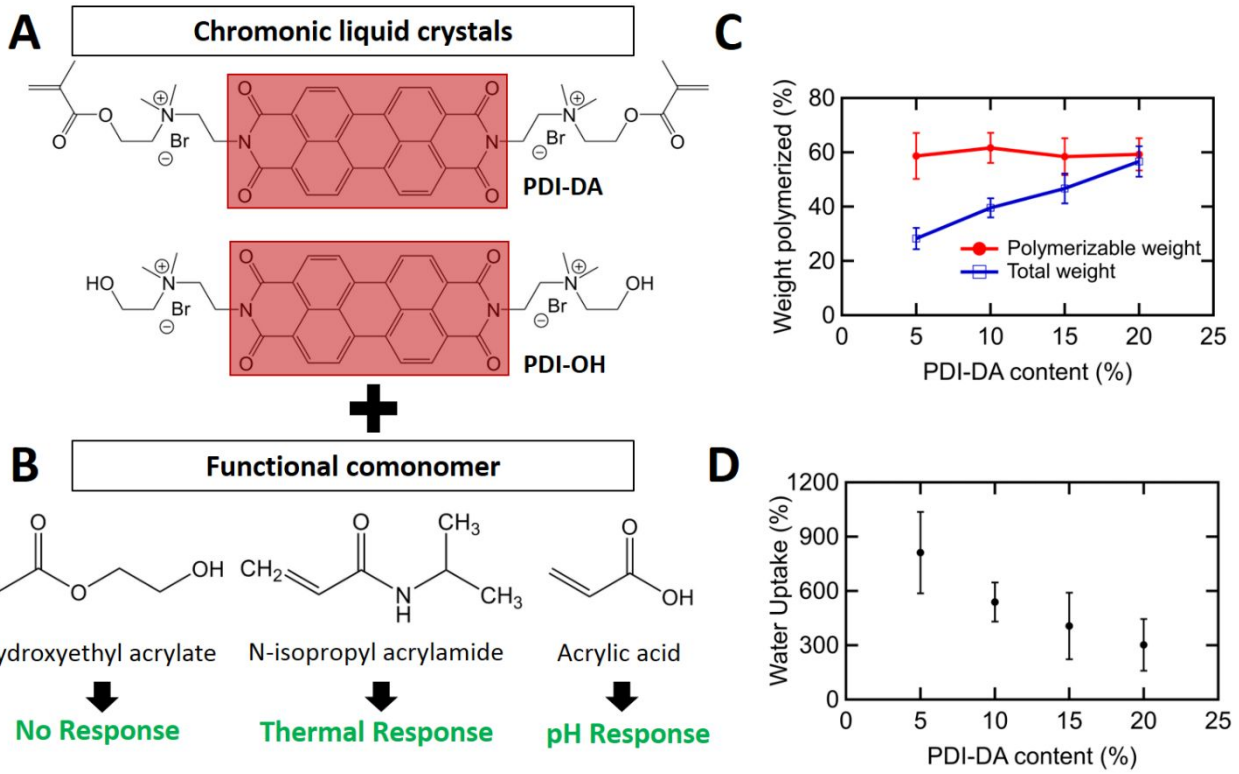

Figure 1. (A) Structures of chromonic molecules perylene diimide dimethacrylate (PDI-DA) and perylene diimide hydroxyl (PDI-OH). (B) Structures of hydrophilic, acrylic comonomers chosen for their responsive properties. (C) Amount of weight converted in polymers of varying crosslink density (as modulated by PDI-DA content) normalized to the initial polymerizable or non-polymerizable content. (D) Amount of water swelled into dry chromonic hydrogels with varying PDI-DA content. Error bars represent standard deviation.

controlling liquid crystal orientation in lyotropic liquid crystals remains a significant challenge.

Chromonic liquid crystals are a subclass of lyotropic liquid crystals which offer better control over molecular order. Chromonic liquid crystals are characterized by flat, hydrophobic cores and ionic groups on the periphery of the molecule. In water, the flat cores stack face-to-face to minimize interaction with water, and the polar groups on the periphery afford solubility in water. These stacks of chromonic molecules exhibit liquid crystalline phases, and their orientation can be controlled by mechanical shear and patterned surfaces, similarly to hydrophobic liquid crystals.[34–36] Until recently, these chromonic liquid crystals had not been used to make polymers due to the absence of chromonic molecules with crosslinkable moieties. The first chromonic hydrogel, polymerized from a newly synthesized chromonic molecule, was recently shown to have anisotropic shape change in response to aqueous stimuli.[37,38]

Here, we use a chromonic monomer in combination with well-known hydrophilic acrylic monomers to impart responsivity into mechanically anisotropic gels, demonstrating patterned, directional swelling. Significantly, the magnitude of shape change can be controlled without sacrificing liquid crystalline order. The directionality of this swelling can be directly controlled by the chromonic orientation and resulting mechanical anisotropy. Finally, we demonstrate the utility of alignable liquid crystals in confinement-based orientation, which results in gels which actuate with Gaussian curvature.

Results & Discussion

A polymerizable dimethacrylate chromonic monomer with a perylene diimide core (PDI-DA) and a non-polymerizable dihydroxyl chromonic molecule with a perylene diimide core (PDI-OH) form the basis of the anisotropic gels (Figure 1A). The direction of the chromonic stacks (denoted by “n”) can be controlled by grooved molds or by confinement, which translates to spatial anisotropy of the resulting gel. The monomer solution is crosslinked in the ordered, liquid crystalline state to yield an oriented polymer network. In many liquid crystalline networks, a phase transition between the liquid crystalline state and the isotropic state drives shape change. Here, the responsive nature of hydrophilic comonomers drives volume change in aqueous environments, while the anisotropic structure imparted by the liquid crystalline order guides the directionality of the volume change.

The stimulus to which the gel responds is determined by the comonomer chosen (Figure 1B). Hydroxyethyl acrylate (HEA) is a hydrophilic comonomer which is stable over a wide range of temperatures and pH conditions, here used for control gels. N-isopropyl acrylamide (NIPAM) and acrylic acid (AA) are responsive comonomers which are used for their volume change in response to temperature or pH, respectively. Based on the desired properties, one of these comonomers is combined in water with the chromonic molecules and an initiator. Using broadband visible light, this mixture can be polymerized into a network, preserving the directionality of the chromonic stacks.

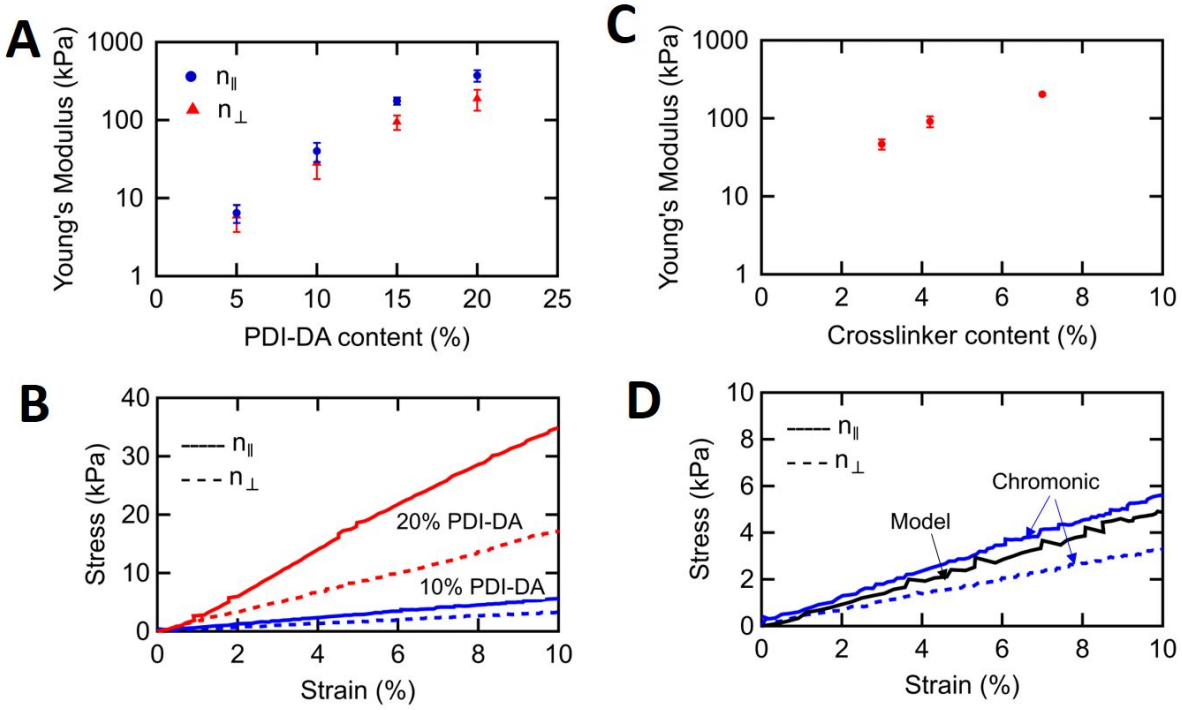

Figure 2. (A) Young's modulus of hydrogels with varying crosslink densities measured along and perpendicular to the chromonic stack direction. (B) Representative tensile curves of chromonic gels with high and low crosslink densities measured along and perpendicular to the chromonic stack direction. (C) Non-chromonic, model gels with variable diacrylate content matching the mechanical properties of corresponding chromonic gels. (D) Representative tensile curves of chromonic hydrogels along and perpendicular to the chromonic stacks as compared to the tensile test of the isotropic model gel of matching mechanical properties. For all figure parts, the solid lines (n‖) represent the direction parallel to the chromonic stacks, and the dotted lines (n⊥) represent the direction perpendicular to the chromonic stacks. Error bars represent standard deviation.

Magnitude of shape change

To control the crosslink density of the gels, we must control the concentration of diacrylate molecules while retaining the liquid crystalline phase. Keeping the total concentration of chromonic constant, the crosslink density is varied by balancing the ratio of polymerizable PDI-DA with non-polymerizable PDI-OH. The chromonic ratio does influence the phase diagram, but the nematic phase is maintained at room temperature for all ratios, as determined by polarizing optical microscopy (POM) (Figure S1). Gels of varying chromonic ratios were copolymerized with HEA in unaligned molds to examine the effect on crosslink density. Crosslinked content is compared between gels by measuring the polymerized weight relative to the monomer weight (Figure 1C). As PDI-OH content increases and PDI-DA content decreases, the gel fraction is reduced. When normalized to only the polymerizable monomers (excluding PDI-OH content), the conversion remains the same for all compositions. This supports the assumption that adding PDI-OH does not affect the polymerization of the other comonomers. Water uptake is measured as another indicator of relative crosslink density (Figure 1D). The water uptake decreases roughly linearly as PDI-DA content increases, which is in agreement with the conversion results.

PDI-DA content directly controls the mechanical properties of the ordered hydrogels. For these experiments, aligned gels were copolymerized with HEA in a mold with uniaxial alignment grooves. Young's modulus was measured by tensile testing of uniaxially aligned gels of varying PDI-DA content on a micromechanical testing machine with an immersion bath (Figure S2). In this setup, the hydrogel film is coupled directly to the bending of a thin beam, which allows for the detection of μN-scale forces. Aligned gels were tested both along and perpendicular to the alignment direction. Modulus is reduced as PDI-DA content is decreased (Figure 2A). By varying the chromonic ratio, we can vary the stiffness of the gels from 6.5 ± 1.7 kPa to 370 ± 62 kPa. Additionally, mechanical anisotropy is retained in gels of all PDI-DA contents, though the anisotropy is reduced for gels with lower crosslink density (Figure 2B). This difference in anisotropy is likely due to the reduction in polymerized liquid crystalline content (Table S1). The gels are stiffer along the chromonic stacks than perpendicular to the stack direction by up to 50% in the stiffest gel. This mechanical anisotropy is key to controlling the resulting shape change.

To determine the contribution of the chromonic phase during polymerization to the observed shape response, we synthesize a model gel by substituting PDI-DA for a hydrophilic crosslinker, poly(ethylene glycol) diacrylate (M_n = 700 g/mol), with similar molecular weight. By varying crosslinker content in the model gels and measuring the stiffness, we created a fit curve to determine the crosslinker content which corresponds to the mechanical properties of chromonic gels at each crosslink density (Figure 2C-D). The amount of crosslinker in the model gels is not equal to the crosslinker content in the chromonic gels likely due to the difference in monomer reactivity and polymerization efficiency. These model gels are used to

elucidate the degree to which the stimulus response of the gel is due to the comonomer or due to the chromonic component.

Type of Stimulus

The stimulus to which the gel responds can be controlled by selecting the appropriate responsive acrylic comonomer. Phase diagrams were generated by varying hydrophilic comonomer concentration (Figure S3). This phase behavior dictates the maximum amount of comonomer in solution for each mixture to be in the nematic, orientable phase at room temperature.

First, we examine the thermal response of chromonic gels copolymerized with NIPAM. To do this, aligned samples of two different crosslink densities were immersed in water and heated to 70 °C (Figure 3A). For gels of both crosslink densities, there is a swollen to deswollen volume transition upon heating due to the lower critical solution temperature of the gel. When the crosslink density is varied from high to low, the magnitude of shape change is considerably increased on average from 18% to 60% along the axis perpendicular to the stack direction. For both crosslink densities, the shape change is anisotropic, which can be attributed to the anisotropic mechanical properties. The chromonic stack axis is slightly stiffer, so less shape change occurs along the stiff, parallel axis than along the more compliant, perpendicular axis. When this shape change is compared to a NIPAM-based model gel without chromonic ordering, the magnitude of shape change is similar, and the anisotropy is no longer present, as expected (Figure 3B). In a chromonic gel copolymerized with HEA instead of NIPAM, we see a minimal anisotropic thermal response, which could be attributed to the minimal thermal response of the comonomer HEA or a weak contribution of from the chromonic monomer (Figure 3C).

To induce a shape change in response to pH, acrylic acid was copolymerized into gels of high and low crosslink density. Poly (acrylic acid) has greater solubility in basic solutions, which results in a large volumetric change in hydrogels formed from this polymer. Aligned samples were placed in acidic or basic conditions, and shape change was evaluated along and perpendicular to the alignment direction. Both high and low crosslink density samples deswelled slightly in acidic conditions and swelled greatly in basic conditions, though at different magnitudes (Figure 4A-B). The lower crosslink density samples had a predictably larger magnitude response to both conditions. The anisotropy is evident in the response of the lower crosslink density sample to basic conditions, where the magnitude of shape change is highest. This shape change is even greater than the shape change in model gels with no chromonic content (Figure 4C). To examine this further, the pH response of chromonic gels copolymerized with HEA, which should be inert to changes in pH, was compared to the response of chromonic gels copolymerized with acrylic acid (Figure 4D).

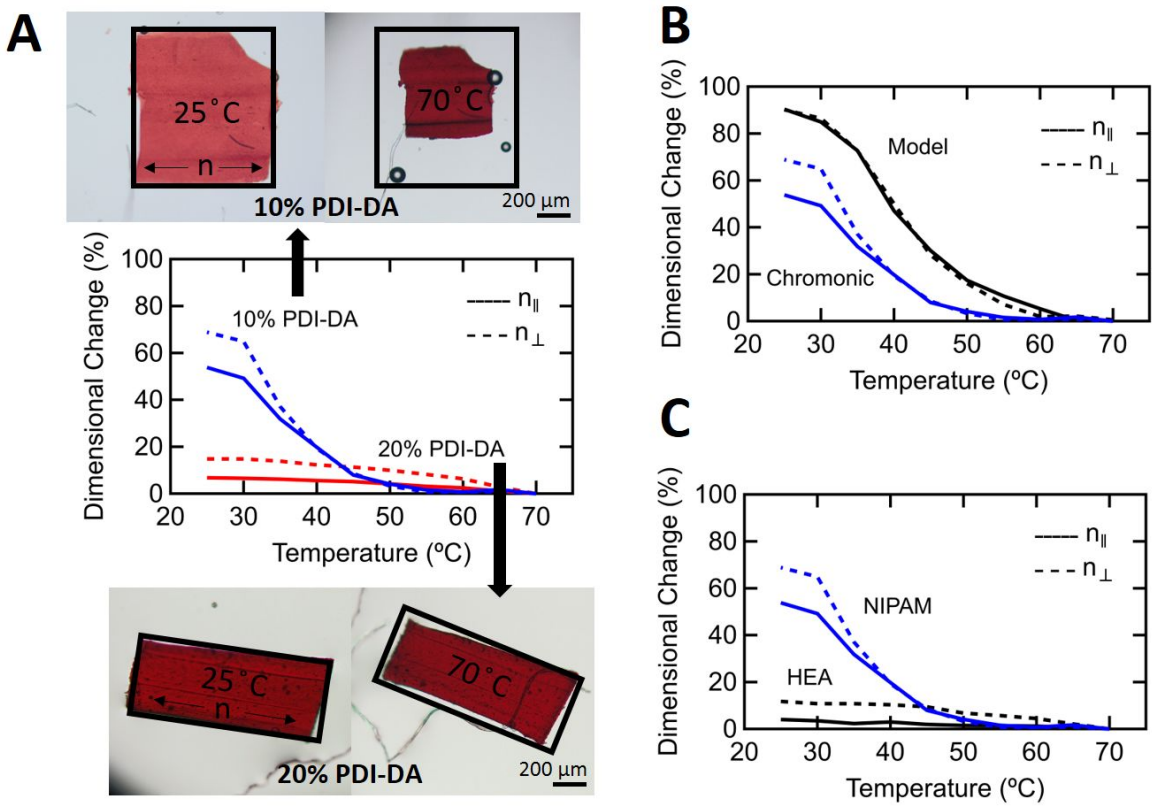

Figure 3. (A) Representative images and curves of high and low crosslink density chromonic hydrogels with NIPAM copolymerized in the system. Dimensional change measured along and perpendicular to the chromonic stacks as a function of temperature. (B) Dimensional change as a function of temperature measured in a low crosslink density chromonic gel and a model, non-chromonic gel with matching crosslink density. (C) Dimensional change as a function of temperature of chromonic gels copolymerized with NIPAM or HEA. For all figure parts, the solid lines (n∥) represent the direction parallel to the chromonic stacks, and the dotted lines (n⊥) represent the direction perpendicular to the chromonic stacks.

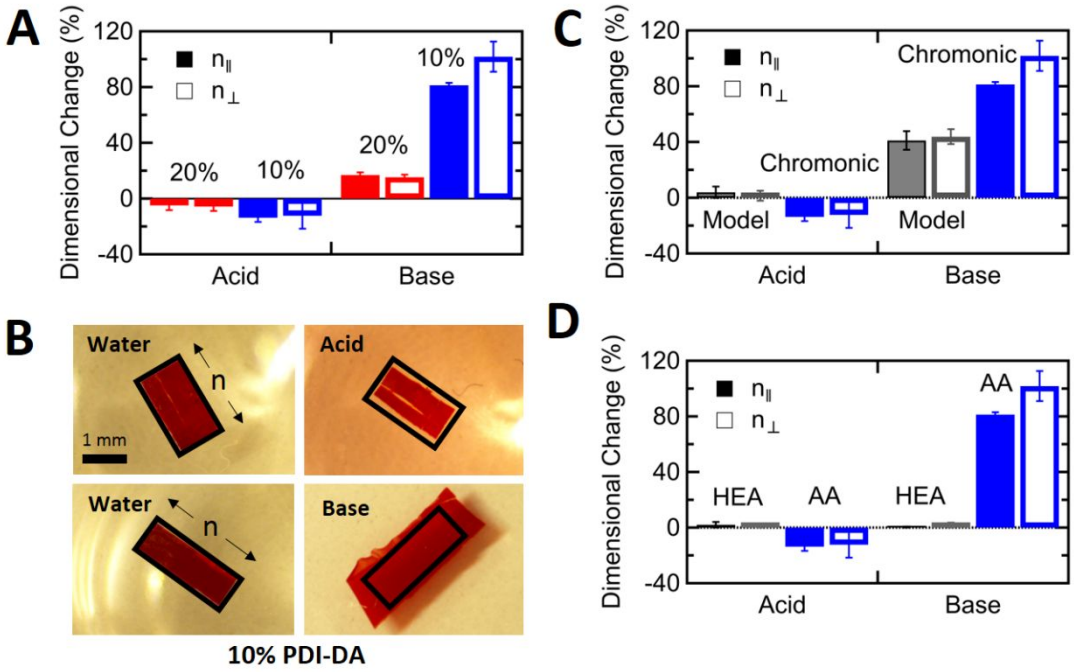

Figure 4. (A) Dimensional change of chromonic hydrogels of high and low crosslink density in pH 4 or pH 9 solutions. (B) Representative images of chromonic hydrogels of high and low crosslink density in pH 4 or pH 9 solutions as compared to neutral solutions. (C) Dimensional change for model acrylic acid hydrogels and chromonic hydrogels of matching crosslink densities in pH 4 or pH 9 solutions. (D) Dimensional change for control HEA gels and chromonic gels of matching crosslink densities in pH 4 or pH 9 solutions. For all figure parts, the solid lines (n‖) represent the direction parallel to the chromonic stacks, and the dotted lines (n⊥) represent the direction perpendicular to the chromonic stacks. Error bars represent standard deviation.

The chromonic gel copolymerized with HEA shows no response to high or low pH, which supports that the quaternary ammonium salt on the chromonic monomer does not significantly contribute to the shape change. We note that ionic interactions between the PDI-DA and the acrylic acid polymer chains could change the pH response profile of the hydrogel.[39,40]

Complex alignment

One of the most interesting features about liquid crystals remains the ability to use self-assembly to control the molecular order. The films discussed thus far have been uniaxially aligned through parallel grooves on a mold surface, but the most compelling demonstration of liquid crystalline order is beyond the size scale which can be patterned by top-down methods, such as rubbing. Though chromonic liquid crystals are notoriously difficult to align, complex, defect-free alignment has been shown through confinement.[41–44] We show that monomer solutions which exhibit chromonic ordering, despite diluted chromonic content due to comonomer presence, both align and polymerize in confined capillaries, retaining complex molecular orientation.

Here, cylindrical and rectangular micron-sized borosilicate capillaries are used as the confining geometry to induce alignment. This alignment can be influenced by the capillary wall anchoring conditions and the additives to the chromonic solution. When the chromonic solution (comonomer acrylic acid, 10% PDI-DA content) is filled into an untreated cylindrical capillary, the stacks orient planarly along the capillary walls and twist towards the center to align along the axis of the tube in a twisted radial configuration (Figure 5A-B). This alignment matches results seen in DSCG both here and in the literature

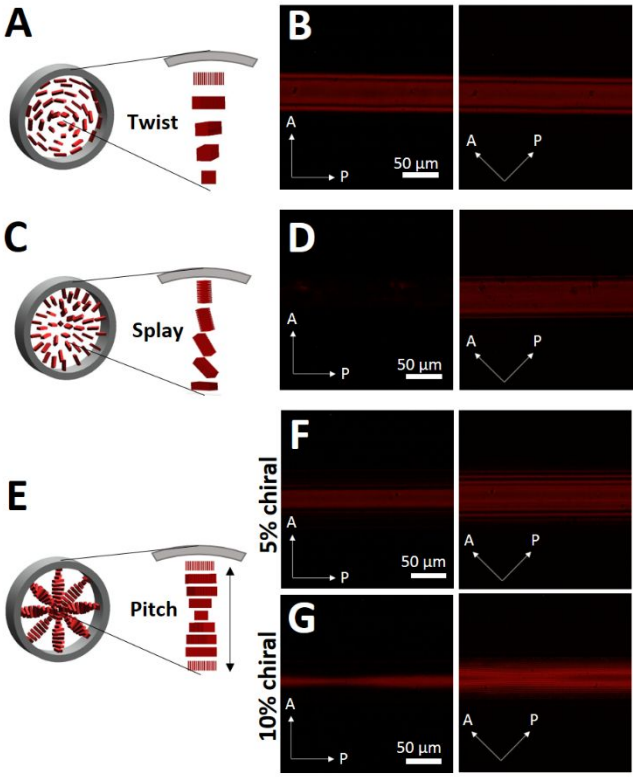

Figure 5. (A) Schematic of molecular order in a capillary with planar wall anchoring (B) POM of a filled capillary with planar wall anchoring positioned along and at 45 °to the polarizers. (C) Schematic of molecular order in a capillary with homeotropic wall anchoring. (D) POM of a filled capillary with homeotropic wall anchoring positioned along and at 45 °to the polarizers. (E) Schematic of molecular order in a capillary with planar wall anchoring and chromonic chiral dopant added. POM images depict filled capillaries with (F) 5% chiral PDI and (G) 10% chiral PDI added.

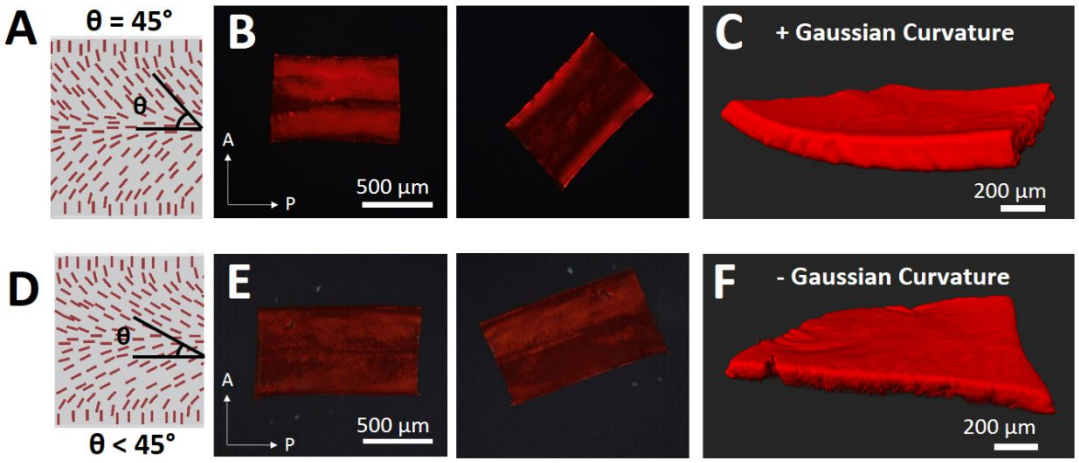

Figure 6. (A, D) Schematics of the stack orientation inside a 50 µm by 500 µm rectangular capillary. (B, E) POM images of the resulting polymer after filling, polymerizing, and etching. (C, F) Fluorescent confocal microscopy images of the polymer immersed in base showing positive or negative Gaussian curvature.

(Figure S4).[41] In the twisted radial configuration, when the alignment is not induced by a chiral dopant of defined handedness, optical boundaries appear between domains of opposite handedness (Figure S5). When the inner capillary walls are treated with hydrophobic, low molecular weight poly(dimethyl) siloxane (Rain-x), the stacks orient homeotropically along the capillary wall and splay towards the center to align along the axis of the tube in an escaped radial configuration (Figure 5C-D). This configuration also matches results seen in DSCG both here and in the literature (Fig S4).[43] To demonstrate alignment at even smaller size scales, varying amounts of a chiral dopant which shares the perylene core (chiral PDI) are added into the polymerizable solution and filled into a cylindrical capillary. The stacks align planarly along the capillary walls and twist towards the capillary center with a pitch proportional to the amount of chiral dopant added (Figure 5E-G).[45] These complex orientations, though not predetermined, are examples of how small changes in the boundary conditions or in solution additives can shift the energetics boundaries enough to alter the stable configuration. Not only do these orientations assemble spontaneously, but these complex, 3D orientations would also be very difficult to achieve by traditional patterning methods.

To create actuating microstructures, we utilize confinement-based ordering in a rectangular capillary. Without treatment, chromonics stack planarly along the capillary wall and splay across the width to align along the capillary axis in the center (Figure 6A, D). Through the bulk of the capillary, the chromonic stacks align at 45° or <45° (commonly 20°-30°) to the capillary axis, which can be visualized using POM by determining the angle at which light extinction occurs (Figure 6B, E). This alignment profile is supported by fluorescent microscopy and by POM with the addition of a quarter waveplate (Figure S6). There does not appear to be any twist or splay along the thickness, and this is supported by the dimensional change in the thickness axis (Figure S7). Notably, this alignment does not match the alignment proposed previously in neat chromonic solutions, but there are many additives in this mixture which may affect the energetic balance of favorable alignment.[42] This alignment pattern produces incompatible strains upon swelling, which causes one axis to bend and the other axis to either bend in the opposite direction, resulting in negative Gaussian curvature or in the same direction, causing positive Gaussian curvature. The type of Gaussian curvature depends on the alignment angle, where angles less than 45° result in Gaussian curvature (θ<45°) and angles around 45° produce positive Gaussian curvature (θ=45°) (Figure 6C, F). A model gel polymerized in the same capillary produces uniform swelling of 40% in all directions with no bending. This outcome is plausible based on previous theoretical research which shows that in similar alignment patterns, negative or positive Gaussian curvatures can emerge based on the alignment angle across the sample.[46,47] This alignment pattern also makes appearances in naturally structured polymers which have been shown to have lyotropic liquid crystal phases, such as collagen, chitin, and cellulose.[48–50] Complex order resulting in Gaussian shape change is a useful tool for multistable actuators, allowing small strains or changes in stimulus to change the configuration of the actuator quickly.

Conclusions

We have demonstrated that we can modify the chemical formulation of chromonic hydrogels to control the resulting shape change in both magnitude and type of response. By including a non-polymerizable chromonic molecule, the magnitude of shape change can be controlled while retaining the benefits of liquid crystalline phase during processing. This results in a wide range of potential materials with tunable stiffness and response magnitude. This chromonic monomer can be mixed with several acrylic comonomers without significantly shifting the phase diagram, which lends to synthetic flexibility and control over the stimulus to which the gel responds. In response to these stimuli, the chromonic ordering lends mechanical anisotropy to the network, which results in anisotropic shape change. We utilize these properties

to create a microstructure which exhibits positive or negative Gaussian curvature in response to basic conditions using emergent molecular order from a confined capillary. These advances in engineering chromonic liquid crystal polymers enable anisotropic hydrogel shape patterning on size scales inaccessible by top-down patterning methods.

Experimental

Materials

Perylene-3,4,9,10-tetracarboxylic dianhydride, N,N-dimethylethylenediamine, 2-bromoethanol, methacrylic anhydride, (S)-(-)-2-aminomethyl-1-ethylpyrrolidine, n-isopropyl acrylamide (NIPAM), hydroxyethyl acrylate (HEA), acrylic acid (AA), hydroquinone, poly(ethylene glycol) diacrylate (PEGDA, M_n=700), potassium persulfate (KPS), sodium hydroxide, fluorescein sodium salt, and 12N hydrochloric acid were purchased from Sigma Aldrich and used without further purification. Dimethylformamide, methanol, dimethyl sulfoxide (DMSO), and tetrahydrofuran (THF) were purchased from Fisher Chemicals and used as received. Irgacure 651 was purchased from Ciba. Glass capillaries were purchased from Vitrocom. Rain-x was purchased from Amazon.com, Inc. Deionized water from ELGA PureLab at 18.2 MΩ purity was used. Cleanroom-grade hydrofluoric acid was provided by the UT Dallas Cleanroom Research Lab.

Synthesis

The synthesis of PDI-DA, PDI-OH, and chiral PDI are described previously.[51,52] Briefly, perylene-3,4,9,10-tetracarboxylic dianhydride and N,N-dimethylethylendiamine were dissolved in DMF and reacted for 12 hrs at 130 °C. Then, the amine-functionalized core is reacted with 2-bromoethanol for 12 hours at 100 °C in DMF to yield PDI-OH. PDI-OH is reacted with methacrylic anhydride in DMF at room temperature for 48 hours catalyzed by 4-dimethylaminopyridine. Chiral PDI is prepared by mixing perylene-3,4,9,10-tetracarboxylic dianhydride with (S)-(-)-2-aminomethyl-1-ethylpyrrolidine in DMSO and stirring at 70 C for 24 hours. The resulting compound is dissolved in concentrated hydrochloric acid before evaporating the acid in a reduced pressure environment to yield chiral PDI. After each synthesis step, the substrate is precipitated in cold THF or methanol and vacuum dried. NMR is run on a Bruker Avance III HD 600 MHz NMR in $CDCl_3$ or D_2O to confirm chemical structure. Phase behavior is observed on an Olympus BX-51 Microscope fitted with polarizers using a Linkam thermal stage.

Film Preparation

Cleaned glass slides were rubbed once with P400 3M sandpaper. Two slides were positioned face-to-face with the grooves parallel and facing inward. The slides were spaced with a 30-60 µm paper spacer secured with a UV-curable thiol-acrylate glue. In the dark, monomers were mixed thoroughly and filled into the mold by capillary action at 40 °C. After filling, the molds were sealed on all sides with thiol-acrylate glue before briefly heating the mold above the isotropic transition temperature (60 °C). Samples were allowed to cool to room temperature. Molds were subsequently placed under broadband white light at an intensity of 35 W/m^2 on a reflective aluminum surface. Molds were flipped frequently for 30 minutes to ensure uniform polymerization. After light exposure, molds were sealed in a humidified container at 85 °C for ~12 hours to postcure. Samples were retrieved from molds and washed in deionized water to remove any unreacted monomers.

Monomer Conversion & Water Uptake

To test monomer conversion, varying amounts of PDI-DA (5%-20%) and PDI-OH (15%-0%) were copolymerized with HEA (10%) using the initiator KPS (1%) in a water solution (69%) (weight percent). Directly after releasing from the mold, samples were cut into 5-10 mg samples, dried, and weighed. After soaking in 5 ml of deionized water for 24 hours to wash out unpolymerized monomer, samples were weighed in the hydrated state. After drying, the sample weight was measured to determine dry mass loss.

Mechanical Testing

For mechanical testing, varying amounts of PDI-DA (5%-20%) and PDI-OH (15%-0%) were copolymerized with HEA (10%) using the initiator KPS (1%) in a water solution (69%) (weight percent). Molds were spaced at 60 µm. Samples (n=3) of 5, 10, 15, and 20% PDI-DA crosslinker with alignment either parallel or perpendicular to the loading axis were cut into 5 mm x 1 mm rectangles. Young's modulus was measured using a tensile setup in a CellScale Microsquisher (Figure S2). In this setup, a tungsten microbeam of 0.2048 mm in diameter is fixed on one end to a vertical actuator. On the opposite end of the beam, a clamp made from a folded 13 µm thick stainless steel sheet is attached and tracked by a camera. In a water bath, samples are loaded into the motorized top clamp and a fixed bottom clamp. The beam was moved at a rate of 10 mm/min, and the beam deflection measured in real time by the relative position of the beam at the camera and at the motor. Force was calculated by the Microsquisher software using the following equation:

$$Deflection = \frac{Force \times Beam\ Length^3}{3 \times Beam\ Modulus\ x\ Beam\ Area\ Moment\ of\ Inertia}$$

The first 5% strain was used to calculate Young's modulus. The anisotropy between the parallel and perpendicular stack axes was determined by the ratio of parallel Young's modulus to the perpendicular Young's modulus. Note that this calculation does not represent the standard deviation of the Young's modulus data, which is represented with the raw data in Figure 2A.

Model gels were made by replacing the chromonic content with PEGDA and matching the mechanical properties to the chromonic gels. Monomers PEGDA (3%, 4.2%, 7%), HEA (10%), Irgacure 651 (1%) and water (86%, 84.8%, 82%) (weight percent) are filled into untreated glass molds spaced at 60 µm. Matching mechanical properties to the chromonic gels at PDI-

DA content of 10%, 15%, and 20% are confirmed by the tensile testing described above.

Thermal Response

To test thermal response, PDI-DA (10% or 20%) and PDI-OH (10% or 0%) were copolymerized with NIPAM (10%) using the initiator KPS (1%) in a water solution (69%) (weight percent). Model thermal gels were made with PEGDA (3% or 7%), NIPAM (10%), Irgacure 651 (1%) and water (86% or 82%). Molds were spaced so that the gap was 30 µm. Samples were cut into 1 mm x 2 mm rectangles, with the stack alignment along the longer axis confirmed by polarizing optical microscopy. Samples were immersed in deionized water and heated from 25 °C to 70 °C on a thermal stage and cooled in ambient air to 25 °C. On the second heating cycle, images were taken every 5 °C on heating and cooling. Images were analyzed in ImageJ to determine the change in length parallel and perpendicular to the stack alignment.

pH Response

For pH response, PDI-DA (10% or 20%) and PDI-OH (10% or 0%) were copolymerized with acrylic acid (9%) using the initiator KPS (1%) in a water solution (70%) (weight percent). Model pH gels were made with PEGDA (3% or 7%), acrylic acid (9%), Irgacure 651 (1%) and water (87% or 83%). Molds were spaced at 30 µm. Samples were cut into ~ 2 mm x 4 mm rectangles with the stack alignment along the longer axis, as confirmed by polarizing optical microscopy. Samples were immersed in deionized water for 24 hours and imaged on an Amscope stereoscope (SM-4B) with an 18MP AmScope digital camera (MU1803-CK). Samples were transferred to an acidic solution (pH 3) prepared with hydrochloric acid in water (0.001 M) for 24 hours and imaged. After equilibrating in deionized water for 8 hours, samples were transferred to a basic solution (pH 9) prepared with sodium hydroxide in water (0.0001 M) for 24 hours and imaged. Images were analyzed in ImageJ to determine the change in length parallel and perpendicular to the stack alignment.

Capillary Preparation

For testing the effect of wall anchoring conditions, a chromonic solution consisting of PDI-DA (10%), PDI-OH (10%), acrylic acid (9%), chiral PDI (0.1%), hydroquinone (0.02%), potassium persulfate (0.1%), and water (70.8%) (weight percent) was prepared. Due to the small size of the capillary, it was necessary to lower the initiator concentration and add the inhibitor hydroquinone in order to allow sufficient time for the chromonic stacks to align before polymerization. The amount of chiral dopant added here was not enough to cause uniform chiral textures, but enough to encourage twist to get a uniform doubly twisted or twisted escaped radial configuration. To achieve planar wall anchoring, no treatment was necessary. Planar capillaries were filled with chromonic solutions by capillary force. For homeotropic wall anchoring, glass capillaries were filled with Rain-x solution by capillary force and dried in an oven at 90 °C overnight. Homeotropic capillaries were filled with chromonic solution by applying suction to one end of the capillary. For evaluating the effect of chiral dopant, a chromonic solution consisting of PDI-DA (10%), PDI-OH (5% or 0%), acrylic acid (9%), chiral PDI (5% or 10%), hydroquinone (0.02%), potassium persulfate (0.1%), and water (70.8%) was prepared. Capillaries were used without treatment and filled by capillary force.

After capillary filling, capillaries were sealed on both ends with epoxy glue and allowed to align in the dark for ~5 minutes before beginning the polymerization. Capillaries were viewed on a polarizing optical microscope while being exposed to <0.1 W/m^2 light filtered at 610 nm. As the PDI cores absorb light, exposure to light causes an energy absorption that drives the nematic phase towards isotropic. Light intensity was slowly increased over ~30 minutes while the orientation was observed. The capillary was flipped multiple times as the solution polymerized to ensure symmetric polymerization. After the light intensity reached 5 W/m^2, if the capillary remained oriented, it was switched to a reflective surface under broadband, white light with intensity 35 W/m^2 for >12 hours. Postcuring was not conducted on these samples as it caused the capillaries to dry out even after extensive sealing, which affected the polymerization. The glass capillaries were etched in 49% hydrofluoric acid for 5 minutes to release the hydrogels and washed thoroughly in deionized water. To observe the hydrogel shape change, capillary samples were immersed in acid (pH = 4, adjusted with HCl) or base (pH = 9, adjusted with NaOH) for >12 hours before imaging and measurement.

Confocal microscopy was performed on an Olympus FV3000RS Laser Scanning Confocal Microscope. Samples were immersed in dilute fluorescein sodium salt solution at pH 9 for approximately 5 minutes before serially washing the sample in base to remove excess dye. Image processing was done in Imaris software.

Conflicts of interest

There are no conflicts to declare.

Acknowledgments

This material is in part based upon work supported by the National Science Foundation under Grant No. 1663367 and the Graduate Research Fellowship Program, Grant No. 1746053. Any opinions, findings, and conclusions or recommendations expressed in this material are those of the author(s) and do not necessarily reflect the views of the National Science Foundation. This work was also funded by the Eugene McDermott Graduate Fellows Program at The University of Texas at Dallas.

The authors would like to thank Revanth Vedula and Abbas Zaki for their contributions to this project.

References

1 A. S. Hoffman, *Adv. Drug Deliv. Rev.*, 2012, **64**, 18–23.

2 X. Du, M. Huang, R. Wang, J. Zhai and X. Xie, *Chem. Commun.*, 2019, **55**, 1774–1777.

3 Y. You, A. T. Nagaraja, A. Biswas, J. Hwang, G. L. Coté and

M. J. McShane, *IEEE Sens. J.*, 2017, **17**, 941–950.
4 S. Ahadian and A. Khademhosseini, *Regen. Biomater.*, 2018, **5**, 125–128.
5 C. A. Custódio, A. del Campo, R. L. Reis and J. F. Mano, in *Woodhead Publishing in Materials*, eds. M. R. Aguilar and J. B. T.-S. P. and their A. (Second E. San Román, Woodhead Publishing, 2019, pp. 411–438.
6 K. S. Soppimath, T. M. Aminabhavi, A. M. Dave, S. G. Kumbar and W. E. Rudzinski, *Drug Dev. Ind. Pharm.*, 2002, **28**, 957–974.
7 D. Gu, A. J. O'Connor, G. G.H. Qiao and K. Ladewig, *Expert Opin. Drug Deliv.*, 2017, **14**, 879–895.
8 S. Haefner, P. Frank, M. Elstner, J. Nowak, S. Odenbach and A. Richter, *Lab Chip*, 2016, **16**, 3977–3989.
9 M. N. Hsu, S.-C. Wei, S. Guo, D.-T. Phan, Y. Zhang and C.-H. Chen, *Small*, 2018, **14**, 1802918.
10 C. Ma, X. Le, X. Tang, J. He, P. Xiao, J. Zheng, H. Xiao, W. Lu, J. Zhang and Y. Huang, *Adv. Funct. Mater.*, 2016, **26**, 8670–8676.
11 Z. J. Wang, C. N. Zhu, W. Hong, Z. L. Wu and Q. Zheng, *J. Mater. Chem. B*, 2016, **4**, 7075–7079.
12 Z. J. Wang, W. Hong, Z. L. Wu and Q. Zheng, *Angew. Chemie Int. Ed.*, 2017, **56**, 15974–15978.
13 Z. L. Wu, M. Moshe, J. Greener, H. Therien-Aubin, Z. Nie, E. Sharon and E. Kumacheva, *Nat. Commun.*, 2013, **4**, 1586.
14 J. Deng, J. Li, P. Chen, X. Fang, X. Sun, Y. Jiang, W. Weng, B. Wang and H. Peng, *J. Am. Chem. Soc.*, 2016, **138**, 225–230.
15 M. Chau, K. J. De France, B. Kopera, V. R. Machado, S. Rosenfeldt, L. Reyes, K. J. W. Chan, S. Förster, E. D. Cranston, T. Hoare and E. Kumacheva, *Chem. Mater.*, 2016, **28**, 3406–3415.
16 A. Sydney Gladman, E. A. Matsumoto, R. G. Nuzzo, L. Mahadevan and J. A. Lewis, *Nat. Mater.*, 2016, **15**, 413.
17 M. Liu, Y. Ishida, Y. Ebina, T. Sasaki, T. Hikima, M. Takata and T. Aida, *Nature*, 2014, **517**, 68.
18 J. Kim, J. A. Hanna, M. Byun, C. D. Santangelo and R. C. Hayward, *Science*, 2012, **335**, 1201 LP-1205.
19 A. Nojoomi, H. Arslan, K. Lee and K. Yum, *Nat. Commun.*, 2018, **9**, 3705.
20 H. Zhang, I. Hussain, M. Brust, M. F. Butler, S. P. Rannard and A. I. Cooper, *Nat. Mater.*, 2005, **4**, 787.
21 J. Zhu, J. Wang, Q. Liu, Y. Liu, L. Wang, C. He and H. Wang, *J. Mater. Chem. B*, 2013, **1**, 978–986.
22 H. Tong, I. Noda and C. C. Gryte, *Colloid Polym. Sci.*, 1984, **262**, 589–595.
23 J. Küpfer and H. Finkelmann, *Die Makromol. Chemie, Rapid Commun.*, 1991, **12**, 717–726.
24 S. Schuhladen, F. Preller, R. Rix, S. Petsch, R. Zentel and H. Zappe, *Adv. Mater.*, 2014, **26**, 7247–7251.
25 T. H. Ware, M. E. McConney, J. J. Wie, V. P. Tondiglia and T. J. White, *Science*, 2015, **347**, 982–984.
26 C. P. Ambulo, J. J. Burroughs, J. M. Boothby, H. Kim, M. R. Shankar and T. H. Ware, *ACS Appl. Mater. Interfaces*, 2017, **9**, 37332–37339.
27 H. Finkelmann, *Angew. Chemie Int. Ed. English*, 1987, **26**, 816–824.
28 T. H. Ware, J. S. Biggins, A. F. Shick, M. Warner and T. J. White, *Nat. Commun.*, 2016, **7**, 1–7.
29 M. Warner and E. M. Terentjev, *Liquid crystal elastomers*, Oxford university press, 2007, vol. 120.
30 J. Jennings, B. Green, T. J. Mann, C. A. Guymon and M. K. Mahanthappa, *Chem. Mater.*, 2018, **30**, 185–196.
31 R. L. Kerr, J. P. Edwards, S. C. Jones, B. J. Elliott and D. L. Gin, *Polym. J.*, 2016, **48**, 635.
32 L. Sievens-Figueroa and C. A. Guymon, *Chem. Mater.*, 2009, **21**, 1060–1068.
33 D. L. Gin, W. Gu, B. A. Pindzola and W.-J. Zhou, *Acc. Chem. Res.*, 2001, **34**, 973–980.
34 J. Y. Kim, K. Nayani, H. S. Jeong, H.-J. Jeon, H.-W. Yoo, E. H. Lee, J. O. Park, M. Srinivasarao and H.-T. Jung, *Phys. Chem. Chem. Phys.*, 2016, **18**, 10362–10366.
35 C. Peng, Y. Guo, T. Turiv, M. Jiang, Q.-H. Wei and O. D. Lavrentovich, *Adv. Mater.*, 2017, 1606112.
36 Y. Guo, M. Jiang, C. Peng, K. Sun, O. Yaroshchuk, O. Lavrentovich and Q.-H. Wei, *Crystals*, 2017, **7**, 8.
37 P. Im, D.-G. Kang, D.-Y. Kim, Y.-J. Choi, W.-J. Yoon, M.-H. Lee, I.-H. Lee, C.-R. Lee and K.-U. Jeong, *ACS Appl. Mater. Interfaces*, 2015, **8**, 762–771.
38 R. S. Kularatne, H. Kim, M. Ammanamanchi, H. N. Hayenga and T. H. Ware, *Chem. Mater.*, 2016, **28**, 8489–8492.
39 Z. E. Ibraeva, M. Hahn, W. Jaeger, A. Laschewsky, L. A. Bimendina and S. E. Kudaibergenov, *Macromol. Mater. Eng.*, 2005, **290**, 769–777.
40 Y. Ogawa, K. Ogawa and E. Kokufuta, *Langmuir*, 2004, **20**, 2546–2552.
41 K. Nayani, R. Chang, J. Fu, P. W. Ellis, A. Fernandez-Nieves, J. O. Park and M. Srinivasarao, *Nat. Commun.*, 2015, **6**, 8067.
42 J. Fu, K. Nayani, J. O. Park and M. Srinivasarao, *NPG Asia Mater.*, 2017, **9**, e393.
43 J. Jeong, L. Kang, Z. S. Davidson, P. J. Collings, T. C. Lubensky and A. G. Yodh, *Proc. Natl. Acad. Sci.*, 2015, **112**, E1837–E1844.
44 Z. S. Davidson, L. Kang, J. Jeong, T. Still, P. J. Collings, T. C. Lubensky and A. G. Yodh, *Phys. Rev. E*, 2015, **91**, 50501.
45 H.-S. Kitzerow, B. Liu, F. Xu and P. P. Crooker, *Phys. Rev. E*, 1996, **54**, 568.
46 C. Mostajeran, *Phys. Rev. E*, 2015, **91**, 62405.
47 M. Cyrus, W. Mark, W. T. H. and W. T. J., *Proc. R. Soc. A Math. Phys. Eng. Sci.*, 2016, **472**, 20160112.
48 Y. Bouligand, *Tissue Cell*, 1972, **4**, 189.
49 I. W. Hamley, *Soft Matter*, 2010, **6**, 1863–1871.
50 D. P. Knight, X. W. Hu, L. J. Gathercole, M. Rusaouën-Innocent, M.-W. Ho and R. Newton, *Philos. Trans. R. Soc. London. Ser. B Biol. Sci.*, 1996, **351**, 1205–1222.
51 R. S. Kularatne, H. Kim, M. Ammanamanchi, H. N. Hayenga and T. H. Ware, *Chem. Mater.*, 2016, **28**, 8489–8492.
52 P. Im, D.-G. Kang, D.-Y. Kim, Y.-J. Choi, W.-J. Yoon, M.-H. Lee, I.-H. Lee, C.-R. Lee and K.-U. Jeong, *ACS Appl. Mater. Interfaces*, 2016, **8**, 762–771.

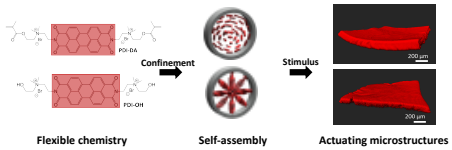
PO-DA
PO-OH
Confinement
Stimulus
200 μm
200 μm
Flexible chemistry
Self-assembly
Actuating microstructures